



Dynamics of a System in a Coupled Duffing and a Ratchet like Potential Functions

Usman A. Marte¹, Sabastine Patrick²

¹Department of Mathematical Sciences, University of Maiduguri, P. M. B. 1069, Nigeria

²Department of Mathematics and Statistics, Federal University of Kashere P.M.B 0182, Gombe, Nigeria

Article Info

Keywords: Coupled Duffing, Ratchet, functions, polynomials

Received 4 March 2024

Revised 17 May 2024

Accepted 22 May 2024

Available online 26 June 2024

<https://doi.org/10.5281/zenodo.12560325>

ISSN-2682-5821/© 2024 NIPES Pub. All rights reserved.

Abstract

This paper considers the dynamics of a system in a coupled Duffing and Ratchet potentials in a range of the position coordinates that captures a complete behaviour for the system so that anything outside this range will only be a repetition because of the periodicity of the system. Due to computational difficulty of the ratchet potential a power series approximation method is applied to transform this part of the potential function to a very closely fitting polynomial so that the entire potential gradient can be uniformly expressed by a polynomial. The positions of all the equilibrium points are evaluated in the range under consideration and the stabilities of all the equilibrium points are obtained from the computation of their eigenvalues. Analytic solutions for the forced and unforced system is found by using two time variable expansion method. The frequency response curve for the system is evaluated for the frequency in the range of [0.0-5.0] the result show stable and unstable response amplitudes obtained by using simple graphical analysis. Regions where only a single response amplitude are found and region where multi-valued response amplitude's are also seen along with hysteresis and jump phenomenon region. The nature of the solutions for the forced system is seen from the simple graphical analysis of the frequency response equation showing how the system will move around the equilibrium points. The work also show how the equilibrium points move as the forcing amplitude is varied for the undamped case, showing how a pair of equilibrium points move toward each other collide and disappear through a reverse saddle-node bifurcation leaving only a single equilibrium point which remain for all the forcing amplitudes considered. Leading to the conclusion that for the Duffing-ratchet system considered the dynamical behaviour found is very similar to that of the purely Duffing only that for this system there are more equilibrium points in particular two more saddle equilibrium points come up as a result of more potential wells of the system. As a result a more complicated dynamical behaviour is seen. Consequently the advantages obtained from complex dynamics of the Duffing system can be better obtained in this Duffing-ratchet system.

1. Introduction

A lot of attention has been directed toward coupled oscillators [1-20] due the fact that it provides the fundamentals to the modelling of various systems consisting of physical, chemical and biological systems. Work has been done on coupled van der Pol oscillators [1-8], coupled Duffing oscillators

[1, 6, and 11, 17-20] and coupled oscillators for the potential of the Ratchet type has been studied in [21-25]. To our knowledge work has not been done on the system that combines all the Duffing-ratchet potentials, so the aim here is to look into the coupling of the Duffing coupled to a potential of the ratchet type. The system to be considered is of the form with the equation of motion given by:

$$\ddot{x} + x + \epsilon(x - x^3 + \alpha(2\pi \cos(2\pi(x - x_0)) + \pi \cos(4\pi(x - x_0)))) = \epsilon F \cos(\omega t) \quad (1)$$

The overall potential $V(x)$ is given by

$$V(x) = \epsilon \left(\frac{x^2}{2} - \frac{x^4}{4} + \alpha U(x) \right) \quad (2)$$

Where $U(x) = c - [\sin(2\pi(x - x_0)) + 0.25 \sin(4\pi(x - x_0))]$

is the Ratchet potential. Where x_0 is an adjustment parameter to make the minima of the ratchet potential to be at integer values and place one of the minima be at the origin [26]

2.0 The autonomous system

The equation of motion of the autonomous system is given by

$$\ddot{x} + x + \epsilon(x - x^3 + \alpha(2\pi \cos(2\pi(x - x_0)) + \pi \cos(4\pi(x - x_0)))) = 0 \quad (3)$$

In the interval of x from $(-1.0, 1.0)$ the negative potential gradient $\frac{dV}{dx}$ is given by

$$\frac{dV}{dx} = (x - x^3 + \alpha(2\pi \cos(2\pi(x - x_0)) + \pi \cos(4\pi(x - x_0)))) \quad (4)$$

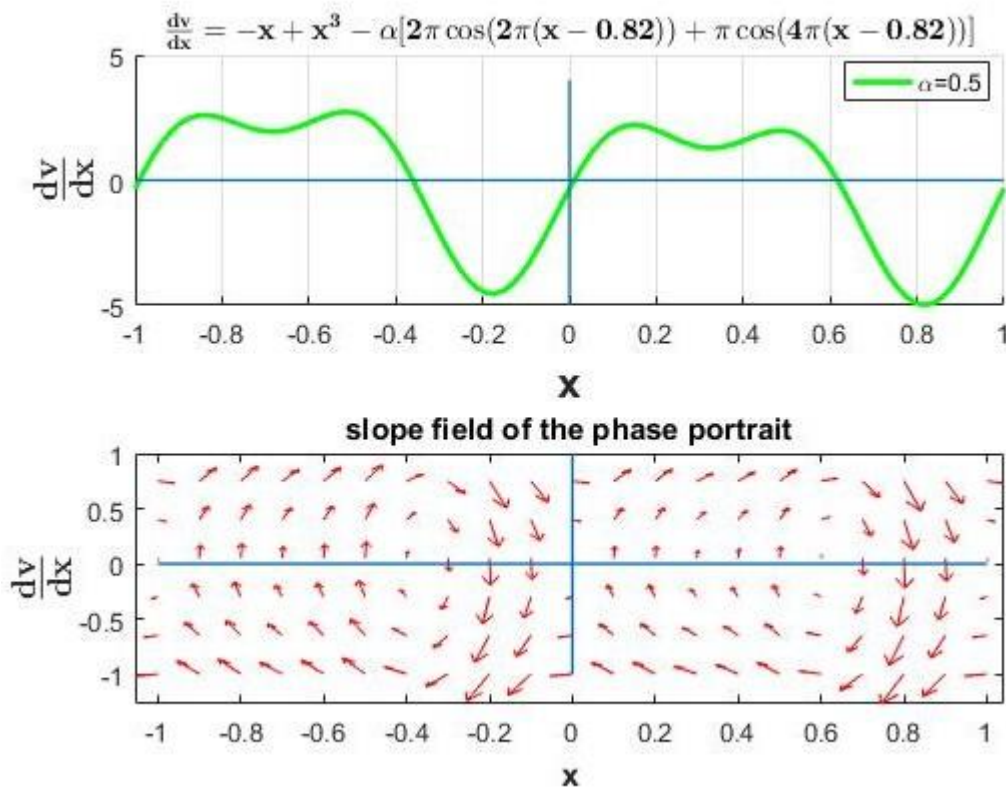


Figure 1: Top figure show the potential gradient as the particle position from -1 to 1 Bottom figure show the slope field for the potential gradient to indicate the nature of equilibrium points

Calculations show that in the interval of [-1.0, 1.0] the system has five EP's at the points given in Table 1.

The Equilibrium points (EQ) for the system under consideration. 5 EQs are seen, their positions and velocities are given in the table.

Table 1: EQ

No	x	v
1	-0.99024	0.0000
2	-0.36068	0.0000
3	0.010696	0.0000
4	0.617278	0.0000
5	1.009740	0.0000

The nature of these equilibrium points (EQ) can also be obtained from the eigenvalues of the Jacobian matrix for around the EQ equilibrium points. The Jacobian matrix denoted by J is given by

$$J = \begin{bmatrix} \frac{\partial f_1}{\partial x} & \frac{\partial f_1}{\partial v} \\ \frac{\partial f_2}{\partial x} & \frac{\partial f_2}{\partial v} \end{bmatrix} = \begin{bmatrix} 0 & 1 \\ \alpha(1 - 3x^2 + 4\pi^2 \beta(\sin(2\pi(x - 0.82)) + \sin(4\pi(x - 0.82)))) & 0 \end{bmatrix} \quad (5)$$

The eigenvalues is given in Table 2.

To their positions and velocities given in Table 1.0 their eigenvalues are added in this table showing centers and saddle EQ's as seen in the slope field in Figure 1.

Table 2: Eigenvalues

No	x	v	Eigenvalues
1	-0.99024	0.0000	± 5.473260
2	-0.36068	0.0000	$\pm 5.690990i$
3	0.010696	0.0000	± 5.724550
4	0.617278	0.0000	$\pm 5.48336i$
5	1.009740	0.0000	± 5.462760

From the Table 2, the eigenvalues computed in the interval [-1.0, 1.0] show three saddle equilibrium points (EQ) and two center equilibrium points (EQ) are seen at the points -0.36068 and 0.617278 where the eigenvalues are purely imaginary which are the centers, while the three points with x values at -0.99024, 0.010696 and 1.00974 have real eigenvalues equal in magnitude but opposite in their signs indicating saddle EQ's. Agreeing with the slope field given in the bottom figure of Figure 1.

3.0 The nonautonomous system

The equation of motion for the system with a small perturbing parameter ϵ can be written as a system of three first order equations given by:

$$\dot{x} = v$$

$$\dot{v} = -(x + \epsilon(x - x^3 + \alpha(2\pi \cos[2\pi(x - x_0)] + \pi \cos[4\pi(x - x_0)])) + \epsilon F \cos z \quad (6)$$

$$\dot{z} = \omega$$

Where $z = \omega t$

The forcing term is a 2π periodic function in z. so without loss generality it can be started at the value of $\omega t = 0.5\pi$ and $\alpha = 0.5$

Whose equilibrium points (EQ) is obtained from the roots of the equations

$$v = 0 \tag{7}$$

$$-(x - \epsilon(x - x^3 + \alpha(2\pi \cos[2\pi(x - 0.82)] + \pi \cos[4\pi(x - 0.82)]))) + \epsilon F \cos z = 0$$

3.1 Two Variable Expansion Method

In this section perturbation method is applied to study the dynamical behaviour for the system for a small perturbing parameter ϵ . The method involves two time scales: Scale for the periodic motion itself and a slower time scale involving the approach to the periodic motion. Which can be represented by $\xi = \omega t$ and $\eta = \epsilon t$ called the stretch and slow times respectively. Application of such a method will require a potential function that can be easily manipulated, as it is the potential consists of two parts the Duffing part and the ratchet part the Duffing part causes no difficulty for it involves only a polynomial, but the ratchet part as it is will cause computational difficulty in the sense that for the two variable expansion to be applicable it will lead to the expansion a composite function of a trigonometric function with the two variable expansion, which will involve approximating the trig function in terms of power series then substituting the two variable expansion into the obtained series approximation. This computational difficulty can be shortened by first writing the ratchet form of the potential gradient by a suitable polynomial just as the Duffing part and apply the two variable expansion uniformly. The ratchet potential gradient is replaced by a polynomial that is obtained using the power series expansion method, the fitting is made to as close as computationally possible. The polynomial so obtained is given by:

$$f(x) = -1871.49x^{19} - 1989.10x^{18} + 9723.30x^{17} + 9808.23x^{16} - 23639.73x^{15} + 22031.03x^{14} + 35780.72x^{13} + 29779.45x^{12} - 36902.54x^{11} - 26370.03x^{10} + 26096.23x^9 + 15254.78x^8 - \tag{8}$$

$$12094.01x^7 - 5352.75x^6 + 3392.26x^5 + 953.11x^4 - 516.81x^3 - 52.65x^2 + 32.07x - 0.34$$

The comparison of the ratchet potential gradient and the approximating polynomial is shown in Figure 2 for the x values in the range $[-1, 1]$.

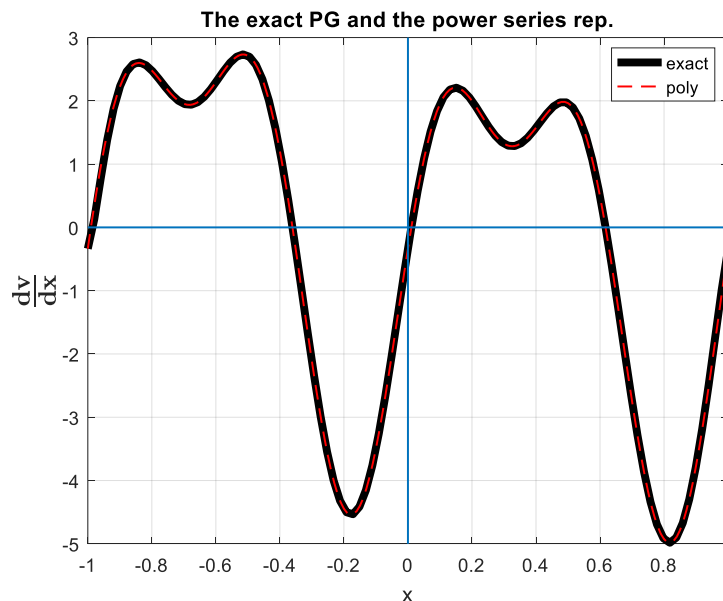


Figure 2: The exact potential gradient (PG) for the system under consideration shown along with the power series representation of the PG

Graph of dv/dx and $f(x)$ drawn on the same axis to show the level of agreement.

The error involved in the computation of the exact potential gradient (PG) and the polynomial approximation for the PG by computing the relative absolute error for x in the interval $[-1:1]$

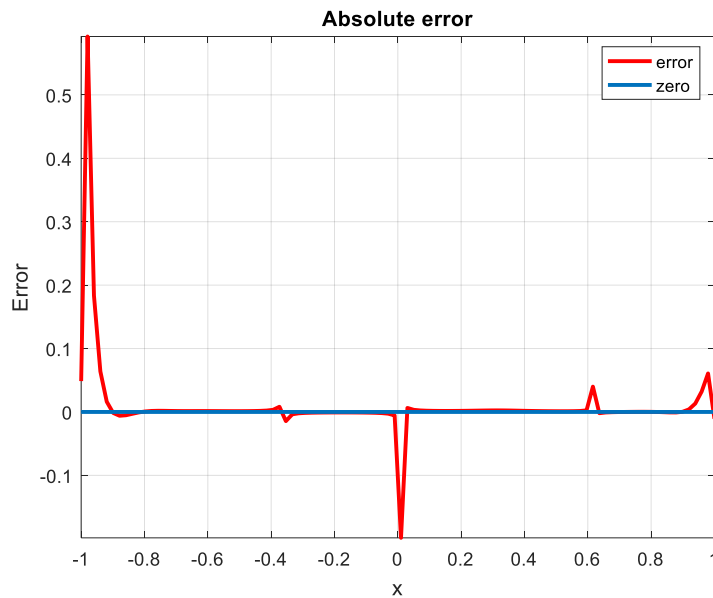


Figure 3: The graph of relative absolute error for the exact PG and the approximate potential gradient

Figure 3 show less than 0.05% relative absolute error everywhere except in a very small interval at the two edges (± 1) and at the origin.

Consider now the two variable exposition method with the stretch time to be given by $\xi = \omega t$ while the slow time to be given by $\eta = \epsilon t$, these definitions to the first and the second derivatives result in

$$\begin{aligned} \frac{dx}{dt} &= \frac{\partial x}{\partial \xi} \frac{d\xi}{dt} + \frac{\partial x}{\partial \eta} \frac{d\eta}{dt} = \omega \frac{\partial x}{\partial \xi} + \epsilon \frac{\partial x}{\partial \eta} \\ \frac{d^2x}{dt^2} &= \omega^2 \frac{\partial^2 x}{\partial \xi^2} + 2\omega \epsilon \frac{\partial^2 x}{\partial \xi \partial \eta} + \epsilon^2 \frac{\partial^2 x}{\partial \eta^2} \end{aligned} \quad (9)$$

Substituting these results into the equation of motion result in

$$\omega^2 \frac{\partial^2 x}{\partial \xi^2} + 2\omega \epsilon \frac{\partial^2 x}{\partial \xi \partial \eta} + \epsilon^2 \frac{\partial^2 x}{\partial \eta^2} + x + \epsilon c \left(\omega \frac{\partial x}{\partial \xi} + \epsilon \frac{\partial x}{\partial \eta} \right) - \epsilon \alpha (x - x^3 + 0.5(u)) = \epsilon F \cos \lambda \quad (10)$$

Where $u(x) = \pi \cos(2\pi(x - 0.82)) + \frac{\pi}{4} \cos(4\pi(x - 0.82))$

Expand x and ω in power series:

$$\begin{aligned} x(\xi, \eta) &= x_0(\xi, \eta) + \epsilon x_1(\xi, \eta) + \dots \\ \omega &= 1 + \kappa_1 \epsilon + \dots \end{aligned} \quad (11)$$

Substitution and neglecting terms of $O(\epsilon^2)$ results in

$$\begin{aligned} \frac{\partial^2 x_0}{\partial \xi^2} + x_0 &= 0 \\ \frac{\partial^2 x_1}{\partial \xi^2} + x_1 &= -2 \frac{\partial^2 x_0}{\partial \xi \partial \eta} - 2\kappa_1 \frac{\partial^2 x_0}{\partial \xi^2} - c \frac{\partial x_0}{\partial \xi} - \alpha (x - x^3 - u(x)) + F \cos(\xi) \end{aligned} \quad (12)$$

The general solution of the first equation of (12) can take the form

$$x_0(\xi, \eta) = A(\eta) \cos(\xi) + B(\eta) \sin(\xi) \quad (13)$$

Where A and B are arbitrary functions of the slow time scale ρ

Substituting into the 2nd equation results in

$$\frac{\partial^2 x_1}{\partial \lambda^2} + x_1 = (\dots) \sin \xi + (\dots) \cos \xi + \text{nonresonant terms} \quad (14)$$

The coefficients of the $\cos \xi$ and $\sin \xi$ are given respectively by

$$2\frac{dA}{d\eta} + cA + 2\kappa_1 B - \frac{3}{4}\alpha BC^2 = 0 \quad (15)$$

$$2\frac{dB}{d\eta} + cB - 2\kappa_1 A + \frac{3}{4}\alpha AC^2 = F \quad (16)$$

Where

$$C^2 = \frac{46189}{131072} A^{18} + \frac{415701}{141072} A^{16} B^2 + \frac{415701}{32768} A^{14} B^4 + \frac{969969}{32768} A^{12} B^6 + \frac{2909907}{65536} A^{10} B^8 + \frac{2909907}{65536} A^8 B^{10} \\ + \frac{969969}{32768} A^6 B^{12} + \frac{415701}{32768} A^4 B^{14} + \frac{415701}{141072} A^2 B^{16} + \frac{46189}{131072} B^{18} \quad (17)$$

The equilibrium points for the slow flow correspond to the periodic motion for the system under consideration. Which can be obtained by setting $\frac{dA}{d\xi} = \frac{dB}{d\eta} = 0$

Resulting in

$$cA + 2\kappa_1 B - \frac{3}{4}\alpha BC^2 = 0 \\ cB - 2\kappa_1 A + \frac{3}{4}\alpha AC^2 = F \quad (18)$$

Multiplying the first equation by B and adding it 2nd equation multiplied by A results in

$$cR^2 = BF \quad (19)$$

Where $R^2 = (A^2 + B^2)$

Again by multiplying the 1st equation by A and subtracting it from the 2nd equation multiplied by B results in

$$\frac{3}{4}\alpha R^2 C^2 - 2\kappa_1 R^2 = AF \quad (20)$$

Adding the squares of the two equations above result in

$$c^2 R^4 + R^4 \left(\frac{3}{4}\alpha C^2 - 2\kappa_1 \right)^2 = R^2 F^2 \quad (21)$$

$$c^2 + \left(\alpha C^2 - 2\kappa_1 \right)^2 = \frac{F^2}{R^2}$$

$$\kappa_1 = \frac{1}{2} \left(\frac{3}{4}\alpha C^2 \mp \sqrt{\frac{F^2}{R^2} - c^2} \right) \quad (22)$$

$$\therefore \omega = 1 + \epsilon \frac{3}{8}\alpha C^2 \pm \frac{1}{2} \epsilon \sqrt{\frac{F^2}{R^2} - c^2} \dots \quad (23)$$

From (15) if the forcing function F and the damping coefficient c are set to zero, then the angular frequency ω is a single valued function, while for both F and c positive and $R < F/c$ ω is double valued function of R.

From (18) and (19) the equilibrium for the undamped system can be written as

$$-2\kappa_1 B + \frac{3}{8}\alpha BC^2 = 0 \quad (24)$$

$$2\kappa_1 A - \alpha AC^2 + F = 0$$

From which it can be found that,

$$B = 0$$

$$A = \pm R \tag{25}$$

$$\kappa_1 = \frac{3}{8} \alpha C^2 \pm \frac{F}{2R}$$

$$\text{With } \omega = 1 + \epsilon \kappa_1 = 1 + \epsilon \left(\alpha C^2 \pm \frac{F}{2R} \right) \tag{26}$$

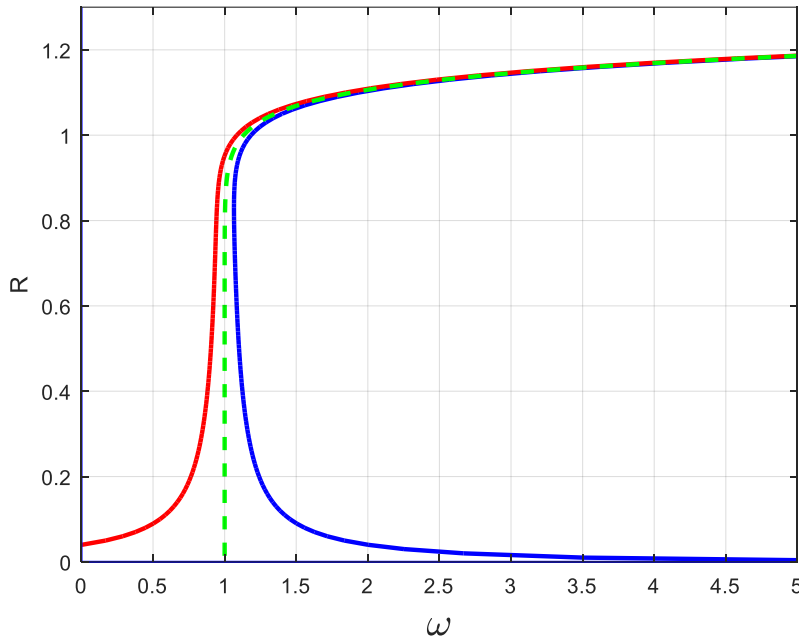


Figure 4: The frequency response curve R on the y axis as function of the forcing frequency ω ranging in the range of 0.0 to 2.0 on the x axis

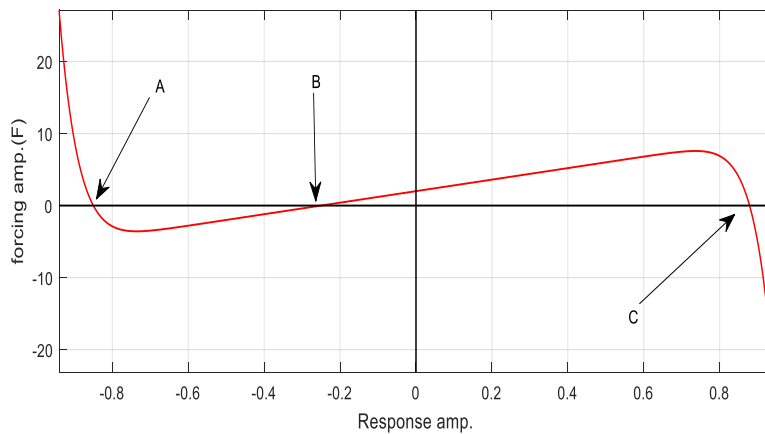


Figure 5: With $\kappa_1 = 3.0$, $F = 2.0$ and $\alpha = 100$ showing three equilibrium points at $A = -0.8825$, $B = -0.3335$ and $C = 0.9216$

The frequency response equation as a function of the response amplitude A , the function f here is given by:

$$f(A) = F + 2\kappa_1 A - \frac{3}{4} \alpha A C^2 \tag{27}$$

From (16) the equilibrium solution with zero damping is plotted against the response amplitude as shown in Figure 5. Qualitatively from the graph the nature of the equilibrium points are obtained from the graphical analysis, i.e. from figure 5.0 it is seen that $f(x)$ to the left of A is positive indicating any particle to left of A move to the right, and to the right of A, $f(x)$ is negative indicating that any particle placed a little to the right of A will move to the left toward A indicating that the point A is a stable center. Similar argument can be applied to the points B and C to see that B is unstable saddle point while the point C is another stable center fixed point.

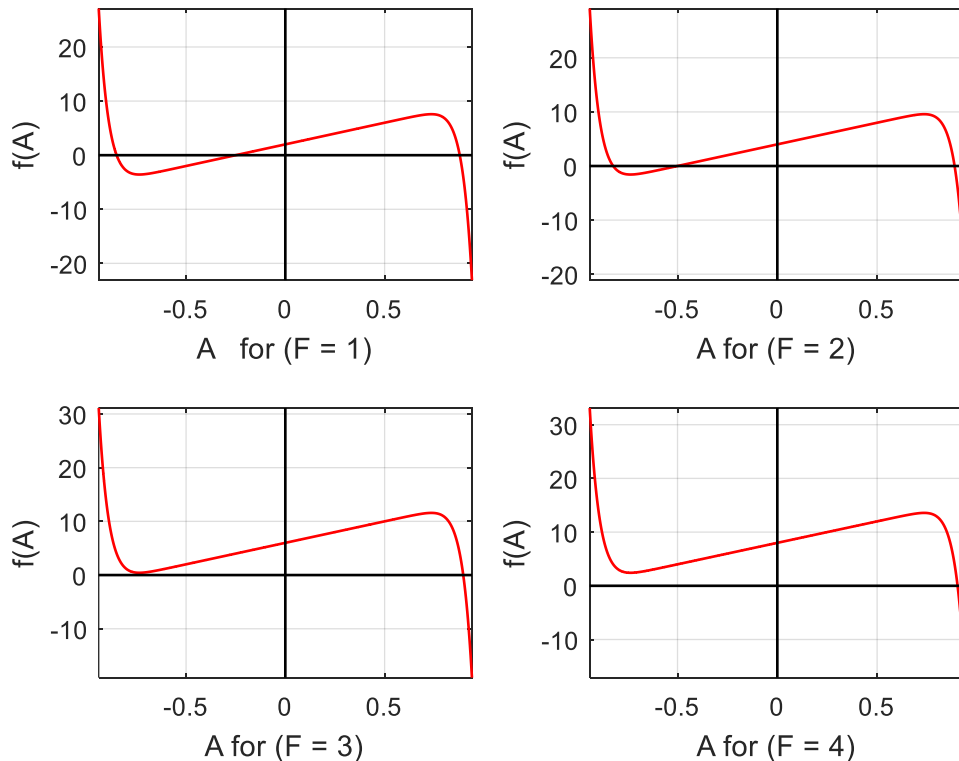


Figure 6: With $\kappa_1 = 3.0$, F is varied to show how the two fixed points move with F

4.0. Conclusion

The dynamics of the coupled Duffing-ratchet system is considered for the position coordinate x ranging from $-0.99 < x < 1.01$ the potential gradient was computed and graphed as shown in the top part of Figure 1 along with the slope fields of the equilibrium points (EQP) in the bottom part of the figure. Showing five EQP at the points $P_1(-0.99,0.0)$, $P_2(-0.36,0.0)$, $P_3(-0.01,0)$, $P_4(0.62,0)$ and $P_5(1.01,0)$. The points P_1 , P_3 and P_5 are saddle equilibrium points while the points P_2 and P_4 are centers, contrary to the Duffing system for the same x range of values where only 3 EQP are seen with saddle at the origin and centers at the endpoints (± 1). Obviously the increase in the EQP is due to the increase in the potential wells in the Duffing-ratchet system, in particular the appearance two new saddle points leads to a more complex dynamics. The frequency response curve (FRC) for the forced system with no damping is evaluated, the FRC show a dynamical behaviour similar to the purely Duffing system in the sense that the backbone curve start from $\omega = 1$ only that for this system the Duffing-ratchet the jump phenomenon seen is so sudden with a very wide range of hysteresis region, implying that the response amplitude vary greatly only in a very small region for $\omega = 0.8$ to $\omega = 1.2$ where the response amplitude jump from 0.2 to 1.0. As seen in figure 4.0. The variation of the FRC for $\omega = 0.0$ to $\omega = 5.0$ is presented from which it is seen that for the upper arm the response amplitude vary from 0.04 to 0.2 for $\omega = 0.0$ to $\omega = 0.8$ then comes the sudden jump region i.e. for ω

= 0.8 to $\omega = 1.2$, where the response amplitude jump from 0.2 to 1.0. Then for ω from the value of 1.2 to 5.0 the response amplitude vary slowly from 1.05 to the maximum value of 1.2 asymptotically. For the lower arm two response amplitudes are seen, for ω from the value of 1.1 to 1.5 there is sudden drop in the response amplitude from a value of about 0.99 to about 0.04 then further increase in ω results in an asymptotic decay of the response amplitude from 0.04 to 0.0. In the lower arm another unstable response amplitude is also seen from the figure for ω ranging from 1.1 to 5.0 the response amplitude grow from 0.99 to the value of 1.2 asymptotically. From figure 5.0 and simple graphical analysis of the Duffing-ratchet system for $\kappa_1 = 3.0$, $F = 2.0$ and $\alpha = 100$ there are two stable EQPs at $A = -0.8825$, and $C = 0.9216$ while an unstable EQP at the point $B = -0.3335$. Which can be generalized to the response amplitude shown in figure 4.0 i.e. for the region for multi response amplitude the upper and the lower branches are stable EQPs while the middle branch is an unstable EQP.

Finally, it is seen that as the forcing amplitude is increased uniformly from 1.0 to 4.0 the two of the three fix points move toward each other that is the saddle fixed point at B and the center fixed point at C merge and disappear through the so called the reverse saddle-node bifurcation just like the Duffing system leaving only the center EQP at C. From this work it can be seen that the Duffing-ratchet system is very similar to that of the Duffing system only that the complexity for this system is higher due the fact that two additional saddle EQM appear in the system which will mean that in areas where the advantage of complex dynamics is required the Duffing-ratchet system will make a better choice.

References

- [1] Nayfeh, A. H., & Mook, D. T. (1979). *Nonlinear oscillations*. Wiley.
- [2] Rand, R. H., & Holmes, P. J. (1980). Bifurcations of periodic motions in two weakly coupled Van der Pol oscillators. *International Journal of Non-Linear Mechanics*, 15(4-5), 387-399.
- [3] Chakraborty, T., & Rand, R. H. (1988). The transition from phase locking to drift in a system of two weakly coupled Van der Pol oscillators. *International Journal of Non-Linear Mechanics*, 23(5-6), 369-376.
- [4] Ashin, P., King, G. P., & Swift, J. W. (1990). *Nonlinearity*, 3(3), 585-594.
- [5] Ashin, P., & Swift, J. W. (1994). *Nonlinearity*, 7(3), 925-942.
- [6] Poolianshenko, M., McKay, S. R., & Smith, C. W. (1991). *Physical Review A*, 43(10), 5638-5647.
- [7] Poolianshenko, M., & McKay, S. R. (1991). *Physical Review A*, 44(6), 3452-3460.
- [8] Poolianshenko, M., & McKay, S. R. (1992). *Physical Review A*, 46(9), 5271-5279.
- [9] Pator-Diaz, I., & Lopez-Fraguas, S. A. (1995). *Physical Review E*, 52(2), 1480-1487.
- [10] Kunick, A., & Steeb, W. H. (1985). *Journal of the Physical Society of Japan*, 54(3), 1220-1223.
- [11] Kapitaniak, T., & Steeb, W. H. (1991). *Physics Letters A*, 152(1-2), 33-36.
- [12] Hackl, K., Yang, C. Y., & Cheng, A. H.-D. (1993). *International Journal of Non-Linear Mechanics*, 28(4), 549-562.
- [13] Cheng, A. H.-D., Yang, C. Y., Hackl, K., & Chajes, M. J. (1993). *International Journal of Non-Linear Mechanics*, 28(4), 441-456.
- [14] Astar, K. R. (1992). *International Journal of Non-Linear Mechanics*, 27(6), 947-962.
- [15] Astar, K. R., & Madoud, K. K. (1994). *International Journal of Non-Linear Mechanics*, 29(3), 421-435.
- [16] Cheng, C. (1991). *International Journal of Non-Linear Mechanics*, 26(1), 105-116.
- [17] Omata, S., Yamaguchi, Y., & Shimizu, H. (1988). *Physica D: Nonlinear Phenomena*, 31(3), 397-408.
- [18] Heagy, J. F., Carroll, T. L., & Pecora, L. M. (1994). *Physical Review E*, 50(3), 1874-1885.
- [19] Skeldon, A. C. (1994). *Physica D: Nonlinear Phenomena*, 75(4), 451-470.
- [20] Eisenhammer, T., Hubler, A., Geisel, T., & Luscher, E. (1990). *Physical Review A*, 41(5), 3332-3335.
- [21] Gelfreich, V., & Sharomov, D. K. (1995). *Physics Letters A*, 197(2), 139-144.
- [22] Kapitaniak, T. (1993). *Physical Review E*, 47(4), R2975-R2978.
- [23] Kozlowski, J., Parlitz, U., & Lauterborn, W. (1995). *Physical Review E*, 51(3), 1861-1867.
- [24] Landa, P. S., & Rosenblum, M. G. (1993). *Applied Mechanics Reviews*, 46(8), 414-425.
- [25] Dressler, U. (1988). *Physical Review A*, 38(4), 2103-2109.
- [26] Dressler, U., & Lauterborn, W. (1990). *Physical Review A*, 41(12), 6702-6707.
- [27] Umberger, D. K., Grebogi, C., Ott, E., & Afeyan, B. (1989). *Physical Review A*, 39(9), 4835-4842.
- [28] Jung, J., Kissner, J. G., & Hanggi, P. (1996). *Physical Review Letters*, 76(18), 3436-3439.
- [29] Mateos, J. L. (2000). *Physical Review Letters*, 84(2), 258-261.

- [30] Barbi, M., & Salerno, M. (2000). *Physical Review E*, 62(1), 1988-1994.
- [31] Kenfack, A., Sweetnam, S. M., & Pattanayak, A. K. (2007). *Physical Review E*, 75(5), 056215.
- [32] Kostur, M., Hanggi, P., Talkner, P., & Mateos, J. L. (2005). *Physical Review E*, 72(3), 036210.
- [33] Vincent, U. E., Nana-Nbendjo, B. R., & McClintock, P. V. E. (2013). *Physical Review E*, 87(2), 022913.